BBA - Molecular Basis of Disease 1871 (2025) 167516

Contents lists available at ScienceDirect

BBA - Molecular Basis of Disease

journal homepage: www.elsevier.com/locate/bbadis

Postnatally overfed mice display cardiac function alteration following myocardial infarction

Marie Josse [a], Eve Rigal [a], Nathalie Rosenblatt-Velin [b], Bertrand Collin [c], Geoffrey Dogon [a], Luc Rochette [a], Marianne Zeller [a,d], Catherine Vergely [a,*]

[a] Research Team: Physiopathologie et Epidémiologie Cérébro-Cardiovasculaires (PEC2), Université de Bourgogne, Faculté des Sciences de Santé, 7 Bd Jeanne d'Arc, 21000 Dijon, France
[b] Division of Angiology, Heart and Vessel Department, Centre Hospitalier Universitaire Vaudois and University of Lausanne, Switzerland
[c] Preclinical Imaging and Radiotherapy Platform, Centre Georges-François Leclerc and Radiopharmaceutiques, Imagerie, Théranostiques et Multimodalité (RITM) Team, Institut de Chimie Moléculaire de l'Université de Bourgogne (ICMUB – UMR CNRS 6302), France
[d] Service de Cardiologie, CHU Dijon Bourgogne, France

ARTICLE INFO

Keywords:
Postnatal overfeeding
Myocardial infarction
Heart failure
Echocardiography
Rodents

ABSTRACT

Background: Cardiovascular (CV) pathologies remain a leading cause of death worldwide, often associated with common comorbidities such as overweight, obesity, type 2 diabetes or hypertension. An innovative mouse model of metabolic syndrome induced by postnatal overfeeding (PNOF) through litter size reduction after birth was developed experimentally. This study aimed to evaluate the impact of PNOF on cardiac remodelling and the development of heart failure following myocardial infarction.
Methods: C57BL/6 male mice were raised in litter adjusted to 9 or 3 pups for normally-fed (NF) control and PNOF group respectively. After weaning, all mice had free access to standard diet and water. At 4 months, mice were subjected to myocardial infarction (MI). Echocardiographic follows-up were performed up to 6-months post-surgery and biomolecular analyses were carried-out after heart collection.
Findings: At 4 months, PNOF mice exhibited a significant increase in body weight, along with a basal reduction in left ventricular ejection fraction (LVEF) and an increase in left ventricular end-systolic area (LVESA), compared to NF mice. Following MI, PNOF mice demonstrated a significant decrease in stroke volume and an increased heart rate compared to their respective initial values, as well as a notable reduction in cardiac output 4-months after MI. After 6-months, left ventricle and lung masses, fibrosis staining, and mRNA expression were all similar in the NF-MI and PNOF-MI groups.
Interpretation: After MI, PNOF mice display signs of cardiac function worsening as evidenced by a decrease in cardiac output, which could indicate an early sign of heart failure decompensation.

1. Introduction

Epidemiological and experimental studies consistently highlight the pivotal role of the foetal and postnatal environment in shaping long-term adult health [1–3]. This concept, termed Developmental Origins of Health and Disease (DOHaD) or neonatal programming emphasizes that during intra-uterine and early postnatal life, organisms are sensitive to hormonal or nutritional stimuli, resulting in significant and sustainable changes in gene expression [4]. However, if the postnatal environment does not match the genomic expression later in life, these

Abbreviations: β-MHC, β-myosin heavy chain; ANF, atrial natriuretic factor; BNP, brain natriuretic peptide; CO, cardiac output; Col1α1, collagen 1α1; Col1α2, collagen 1α2; cTnT, cardiac troponin T; CV, cardiovascular; HR, heart rate; ipGTT, intraperitoneal glucose tolerance test; ipITT, intraperitoneal insulin tolerance test; IS, infarct size; IZ, infarcted zone; LVEF, left ventricular ejection fraction; LVESA, left ventricular end-systolic area; LVEDA, left ventricular end-diastolic area; LVESV, left ventricular end-systolic volume; LVEDV, left ventricular end-diastolic volume; MI, myocardial infarction; NF, normal feeding; PSLA, parasternal long axis; PNOF, postnatal overfeeding; RT-qPCR, reverse transcription-quantitative polymerase chain reaction; RZ, remote zone; SV, stroke volume; TTE, transthoracic echocardiography.

* Corresponding author.
E-mail addresses: marie.josse@u-bourgogne.fr (M. Josse), eve.rigal@u-bourgogne.fr (E. Rigal), nathalie.rosenblatt@chuv.ch (N. Rosenblatt-Velin), bertrand.collin@u-bourgogne.fr (B. Collin), luc.rochette@u-bourgogne.fr (L. Rochette), marianne.zeller@u-bourgogne.fr (M. Zeller), cvergely@u-bourgogne.fr (C. Vergely).

https://doi.org/10.1016/j.bbadis.2024.167516
Received 12 February 2024; Received in revised form 11 September 2024; Accepted 12 September 2024
Available online 18 September 2024

changes may become inappropriate, predisposing individuals to the development of metabolic or cardiovascular (CV) diseases [5,6].

Experimentally, a model of postnatal overfeeding (PNOF) was developed in rodents through litter size reduction after birth. This model, designed to increase neonate's nutritional intake by enhancing milk accessibility, induces significant changes in body weight at weaning, persisting into later adulthood [7]. PNOF-induced overweight is also associated with metabolic impairments, including glucose intolerance, insulin resistance and elevated cholesterol and triglycerides levels, indicative of a metabolic syndrome status [8–11]. Regarding the CV function, PNOF animals display increased cardiac hypertrophy, elevated blood pressure and fibrosis, along with decreased vasodilatory capacities [12–16].

Overweight and obesity-associated metabolic syndrome is a well-recognized risk factor of CV pathologies including myocardial infarction (MI) [17,18]. Following MI, the heart undergoes profound remodelling involving the infarcted zone, marked by collagen production for the fibrotic scar formation [19–22], and the remote zone characterized by myocyte hypertrophy and dilation of the left ventricle [21,23]. This cardiac remodelling process, aimed at compensating for cardiomyocyte death and maintaining adequate cardiac output, becomes deleterious over time and results in the development of heart failure [23,24]. Progression towards heart failure is accompanied by the impairment of systolic and/or diastolic function and a gradual loss of the ability to sustain the organism's needs for blood and oxygen, leading to clinical symptoms and, ultimately, death [25].

In previous works, our research team observed that mice raised in PNOF conditions displayed higher sensitivity to cardiac stressful challenges, such as *ex vivo* ischemia-reperfusion injury [7] and chemotherapies with potential cardiotoxicity [26]. Based on these findings, we hypothesized that PNOF may induce a predisposition to the development of post-MI heart failure in adult mice. The aim of this study was to assess the impact of PNOF on heart failure development after experimentally induced-myocardial infarction in adult mice.

2. Material and methods

2.1. Postnatal overfeeding

All animals received care according to the institution's guidelines. Female and male C57BL6/J mice (Charles River, L'Arbresle, France) were mated in individual cages with *ad libitum* access to water and food. Females were housed separately in individual cages throughout gestation and lactation. After birth, on the second day of life, male pups were randomly distributed among mothers to form the two experimental groups: the control group, normally fed (NF), consisted of 9 pups per litter while the overfed group submitted to postnatal overfeeding (PNOF) comprised 3 pups per litter, as reported previously [15]. It has been previously described that 4-months-old PNOF males were more susceptible to ischemia-reperfusion injury compared to PNOF females, which is why only males were selected for this study. Twenty-four days after birth, the mice were weaned and chipped for identification. They were then housed in cages with *ad libitum* access to standard food and water.

2.2. Experimental protocol

The experimental protocol is described in Fig. 1. At 4 months after birth, baseline parameters of cardiac function were measured through echocardiography in mice from NF and PNOF groups. Subsequently, *in vivo* cardiac surgery was performed to induce experimental myocardial infarction, creating the NF-MI and PNOF-MI groups. Echocardiographic follows-up were conducted every month for 6 months post-surgery using the Vevo 3100 (Fujifilm VISUAL SONICS). At 6 months post-MI, the left ventricle and the lungs were harvested for weighing to determine cardiac mass, corresponding to left ventricular mass on tibia length ratio, and to identify signs of pulmonary congestion. The left ventricle was divided into two distinct zones: the remote zone (RZ) and the infarcted zone (IZ). Cardiac tissues were frozen at −80 °C for gene expression studies or preserved in 4 % PFA for histological analyses.

Prior to the current study, a similar protocol was conducted (Supplementary data, Fig. S1). At 4 months old, mice from NF or PNOF groups underwent either sham surgery (NF-Sham and PNOF-Sham) or myocardial infarction (NF-MI group and PNOF-MI group). Echocardiographic follows-up were performed at 7 days, 1, 1.5 and 2 months after surgery using Vevo 770 (Fujifilm VISUAL SONICS). Following heart collection, gene expression in the RZ and IZ was also evaluated.

After birth, new-born mice were distributed into the NF group, consisting of 9 pups per litter, or the PNOF group composed of 3 pups per litter. At 24 days old, mice were weaned and given standard diet for the remainder of the protocol. At 4 months old, basal transthoracic echocardiography (TTE) was performed, followed by *in vivo* cardiac surgery to induce myocardial infarction. TTE follow-ups were conducted up to 6 months post-MI using the Vevo 3100 echograph. At the end of the protocol, the heart was harvested and divided into 2 zones, the remote zone and the infarcted zone, for histological and RT-qPCR analyses. NF, normally fed group; PNOF, postnatally overfed group; TTE, transthoracic echocardiography.

2.3. Glycemia tests: ipGTT and ipITT

In a distinct series of mice, intraperitoneal glucose tolerance test (ipGTT) and insulin tolerance test (ipITT) were carried out at 4 months of age in NF and PNOF mice that were not submitted to cardiac surgery. Blood glucose level was measured using a glucometer. All mice underwent a 6 h fasting prior to the tests. For the GTT, as previously described [27], basal glycemia (time 0) was measured from blood droplet collection from the tail vein. An intraperitoneal injection of glucose (2 g kg^{-1}) was administered, and glycemia was measured at 15, 30, 45, 60, 75, 90, 105, and 120 min following the injection. For the ITT, human recombinant insulin (0.75 IU kg^{-1}; Actrapid, Novo Nordisk, France) was injected and blood glucose was measured at the same time points as for the GTT.

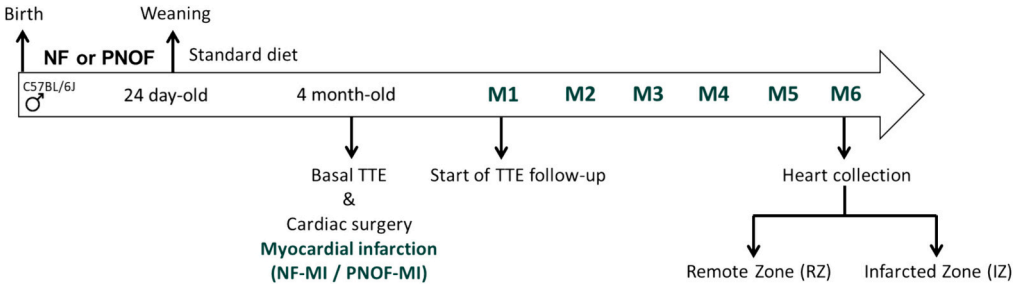

Fig. 1. Schematic view of the experimental protocol.

2.4. In vivo cardiac surgery

At 4 months, NF and PNOF mice underwent surgically-induced MI through permanent ligation of the left anterior descending artery (LAD). Mice were anesthetized using gas mixture of isoflurane (induction at 4 % and surgery at 2.5 %) and oxygen (4.5 l/min) followed by intubation for artificial ventilation (VentElite 55-7040, Harvard Apparatus). Post-intubation, they received an injection of general analgesia (buprenorphine, Buprecare®, 0.075 mg/kg) and topical anesthesia (lidocaine/prilocaine, Anesderm® Ge, 5 %). Electrocardiogram (ECG) and body temperature were continuously monitored throughout the surgery. After shaving, the thorax was opened and the ribs were spread to expose the heart. An 8–0 silk suture was placed and tightened around the LAD. Cardiac ischemia was confirmed by the elevation of the ST segment on the ECG and whitening of the apex area. The rib cage was closed using triple knots with a 5.0 surgical thread. Sham-operated mice underwent a similar surgery without LAD occlusion. A new injection of Buprecare® was administered 2 and 24 h after surgery to maintain analgesic coverage.

2.5. Echocardiography

Transthoracic echocardiography (TTE) was performed using Vevo 3100 devices (Fujifilm VISUAL SONICS), equipped with 40 MHz high frequency transducer. Mice were anesthetized with gas mixture of isoflurane (induction at 4 % and TTE at 2 %) and oxygen (4.5 l/min) and placed in a supine position on a heating pad. Body temperature was monitored with a rectal probe to maintain it between 36 and 37 degrees. Physiological parameters, heart and respiratory rates, and ECG were measured by placing paws on electrodes. The chest was shaved with depilatory cream. The parasternal long axis view (PSLA) was obtained in 2D brightness mode (B-mode) to acquire contractile function parameters. Diastolic parameters were acquired with pulsed wave Doppler (PW-Doppler) and tissue Doppler imaging (TDI). All parameters were measured using Vevo Lab software and averaged from 3 cardiac cycles. Left ventricular end-systolic and -diastolic volumes (LVESV and LVEDV) were evaluated from end-systolic and end-diastolic areas (LVESA and LVEDA) measurements, allowing calculation of the different contractile parameters:

- Stroke volume (SV) (µl): $SV = LVEDV - LVESV$
- Ejection fraction (EF) (%): $EF = (SV/LVEDV) * 100$
- Cardiac output (CO) (ml/min): $CO = SV * (HR/1000)$

E and A waves were measured using PW-Doppler and e′ and a′ waves were measured through TDI for the calculation of E/A ratio and E/e′ ratio.

Infarct size (IS) was determined from B-mode images taken 2 months post-MI, as previously described [28]. This analysis was made at 2 months in order to compare IS between the 2 protocols (2- and 6-motnhs after surgery), and it did not show differences with IS measurement performed 7 days after surgery. Briefly, the total left ventricular end-diastolic area and akinetic area were traced on the same image. The infarct size, expressed as a percentage, was computed using the following formula: - *IS* (%) = *Akinesia length* (mm) / *Total length* (mm) * 100.

Infarct size measurement enabled the identification of exclusion criteria. Mice with an IS <30 % exhibited no discernible signs of cardiac function alterations, while those with an IS >55 % were unable to complete the entire protocol. Consequently, mice falling into these categories were excluded from the study. A flow chart of the two protocols including the initial and final number of mice in each group and the number of mice that did not fall into the inclusion criteria and that died during or after surgery can be seen in Fig. 2 and Supplementary data, Fig. S2.

Initially, 9 mice were included in both NF and PNOF groups. Mice that died during or after the cardiac surgery and mice with infarct size <30 % or >55 % were excluded from the protocol. At the end of the protocol, 5 and 6 mice were included in the NF and PNOF group, respectively. NF, normally fed group; PNOF, postnatally overfed group; IS, infarct size.

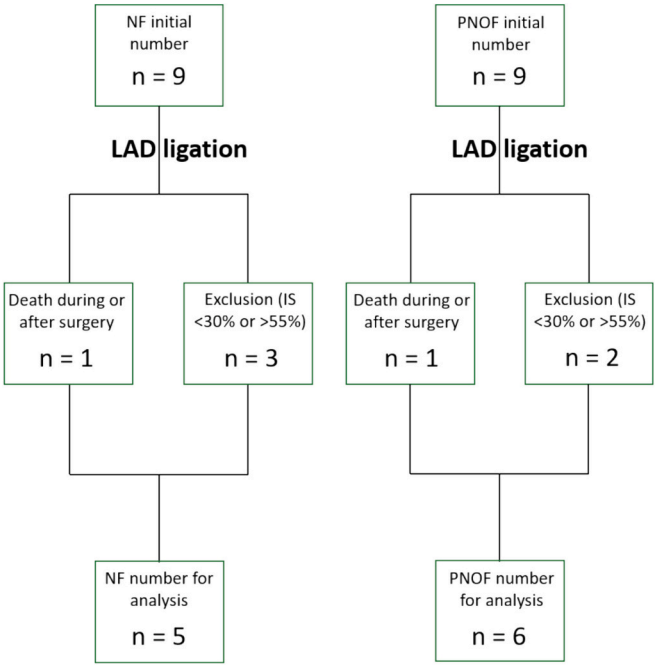

Fig. 2. Flow chart of the study.

2.6. Sirius red staining

The assessment of interstitial cardiac fibrosis in the remote zone was conducted in the ImaFlow core facility (UMR1231-LNC Inserm, University of Burgundy, Dijon, France) with Sirius red staining on deparaffinized cardiac tissue slides. The slides were observed under a white light and polarized light microscope, Axioscope (Zeiss) using the GRYPHAX® software and interstitial fibrosis was analyzed using Image J software. The total tissue surface area and the fibrosis surface were measured using white light images and polarized light images, respectively. The interstitial fibrosis rate was then computed as the ratio of the fibrosis surface area to the total tissue surface area. The fibrosis rate for each animal was determined as the average of 5 images, while the fibrosis rate for each group was represented as the average ± SEM of 5 hearts for the NF-MI group and 6 hearts for the PNOF-MI group.

2.7. RT-qPCR

Gene expression was evaluated through RT-qPCR as previously described [29]. Total RNA from heart tissues at 2- and 6-months post-MI in NF and PNOF mice was extracted using Macherey-Nagel™ NucleoZOL. cDNA synthesis was carried out using PrimeScript™ RT reagent kit (Takara Bio Inc.) and Polymerase Chain Reactions were performed using the SYBR® Premix Ex Taq™ polymerase (Takara Bio Inc.) and StepOnePlus™ Real-Time PCR System (Applied Biosystems). The results were obtained after 40 cycles of a thermal step protocol, including an initial denaturation at 95 °C (15 s), followed by an elongation at 60 °C (1 min) of. Primer sequences are reported in Table 1. Results were obtained as CT values and normalized using the 18S housekeeping gene (Δ CT values). Means of ΔΔ CT values were calculated and results were represented as $2^{-\Delta\Delta CT}$ (fold change). Statistics were performed on ΔΔ CT individual values. SEM fold increase was calculated using $2^{-\Delta\Delta\ CT} - 2^{-\text{means of } \Delta\Delta CT}$.

Table 1
Primer's sequences.

Genes	Forward (5′ to 3′)	Reverse (5′ to 3′)
18S	ACTTTTGGGGCTTCGTGTC	GCCCAGAGACTCATTTCTTCT
ANF	GTGCGGTGTCCAACACAGAT	TCCAATCCTGTCAATCCTACCC
BNP	TTGGGCTGTAACGCACTGAA	TTCAAAGGTGGTCCCAGAGC
Myh7	GCTACGCTTCCTGGATGATCT	CCTCTTAGTGTTGACAGTCTTCC
Troponin T	CAGAGGAGGCCAACGTAGAAG	CTCCATCGGGGATCTTGGGT
Col1α2	GGCCCCCTGGTATGACTGGCT	CGCCACGGGGACCACGAATC
Col1α1	AATGGCACGGCTGTGTGCGA	AACGGGTCCCCTTGGGCCTT

2.8. Cardiac troponin I assay

Circulating cardiac troponin I (cTnI) levels were assessed in plasma collected from NF and PNOF mice, 24 h post-MI. The assay was carried out using enzyme-linked immunosorbent assay (ELISA), utilizing a specific commercial kit (Cloud clone corporation) in accordance with the manufacturer's instructions.

2.9. Statistical analysis

Graphs and statistical analyses were performed on Sigma plot (version 12.5, Systat Software). For statistical analysis, normality and equal variance were tested using Shapiro-Wilk and Levene's tests, respectively. When these assumptions were met, differences between two groups were assessed with a Student's *t*-test, otherwise a Mann-Whitney's test was performed. Analysis comparison over time was assessed using Two-Way Repeated Measures ANOVA followed by *post hoc* Holm-Sidak's multiple-comparison tests. A p-value < 0.05 was considered statistically significant.

3. Results

3.1. Body weight

Myocardial infarction did not exert a significant effect on the body weight of mice, as evidenced by the comparable weights of MI-operated mice and their respective sham-operated controls for up to 2 months post-surgery (Supplementary data, Fig. S3).

The body weight of 4-months-old PNOF-MI mice exhibited a significant 8.5 % increase compared to the NF-MI group (32.5 ± 1.0 g *vs* 30.0 ± 0.3 g; $p < 0.05$) (Fig. 3). Following cardiac surgery, the body weight of PNOF-MI mice remained consistently higher than that of NF-MI mice at 1-, 4-, 5- and 6-months.

3.2. Glucose and insulin tolerance tests

Glucose and insulin tolerance tests were performed at 4 months of age in an independent series of NF and PNOF mice (Fig. 4). PNOF mice displayed a 9.9 % body weight increase compared to NF mice (30.9 ± 0.59 in NF mice *vs* 33.4 ± 0.39 in PNOF mice; $p < 0.05$). The ipGTT revealed an increased glycemia after glucose injection evidenced by a higher incremental area under the curve (+23 %; $p < 0.05$). For the ipITT, we did not observe any difference of area mean under the curve between the two groups.

3.3. Infarct size

Two months post-MI, infarct size (IS) was measured (Fig. 5A). IS values were 40.2 ± 1.8 % for NF-MI and 43.0 ± 2.8 % for PNOF-MI mice, with no significant differences between the two groups.

A significant correlation was found between IS and LVEF (correlation coefficient $r = -0.936$; $p < 0.001$) (Fig. 5B). Mice with infarct sizes <30 % or >55 % were excluded from the protocol, resulting in the exclusion of 3 and 2 mice from NF-MI and PNOF-MI groups, respectively.

In the first protocol, IS values were 41.2 ± 2.6 % for NF-MI and 41.0 ± 2.5 % for PNOF-MI mice (Supplementary data, Fig. S4A). Additionally, 3 mice from NF-MI group and 2 mice from PNOF-MI group were excluded (Supplementary data, Fig. S4B).

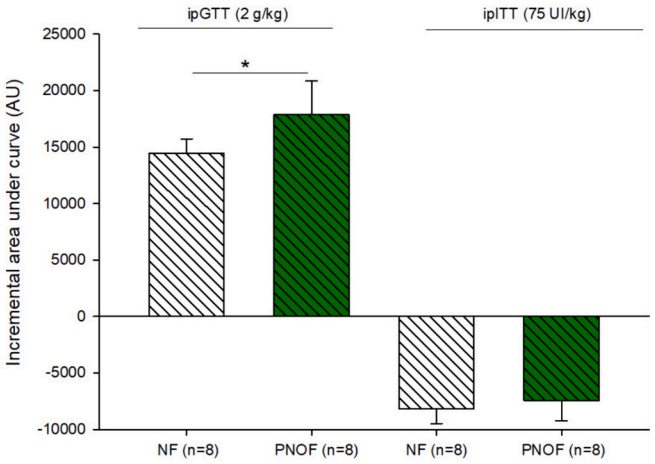

Fig. 4. Incremental area under the curve of blood glucose after intraperitoneal glucose or insulin injection in NF and PNOF mice. *: significantly different from NF mice ($p < 0.05$). Student or Mann-Whitney's test. ipGTT, intraperitoneal Glucose Tolerance Test; ipITT, intraperitoneal Insulin Tolerance Test.

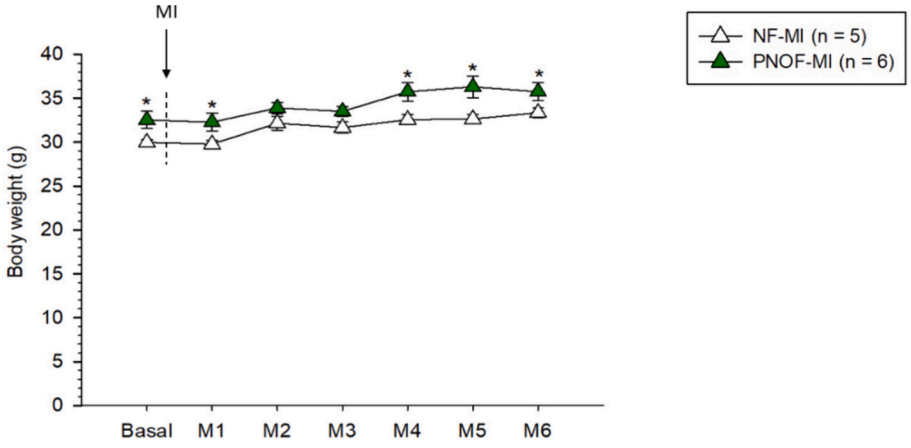

Fig. 3. Body weight evolution of NF-MI and PNOF-MI mice. *: significantly different from NF-Sham mice ($p < 0.05$). Two Way Repeated Measures ANOVA.

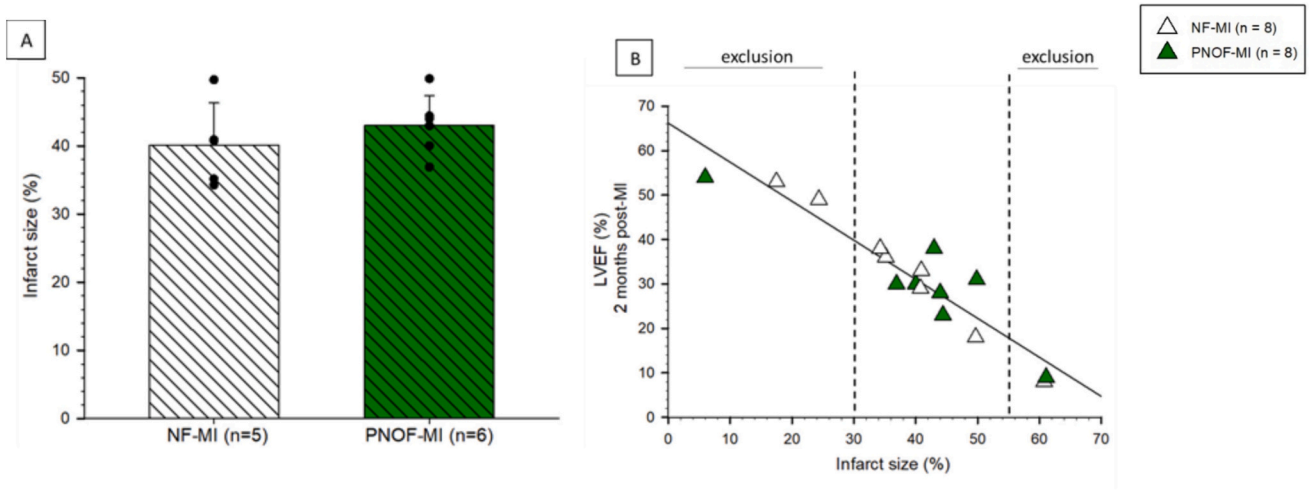

Fig. 5. (A) Infarct size of NF-MI and PNOF-MI mice measured 2 months post-surgery on echograph Vevo 3100. (B) Regression plot of correlation between LVEF and IS of NF-MI and PNOF-MI measured 2 months post-MI and exclusion criteria.

3.4. Left ventricular ejection fraction and areas

LVEF of sham groups remained unaffected by surgery and showed no differences between NF-Sham and PNOF-Sham mice throughout the TTE follow-up (Supplementary data, Fig. S5A). Similarly, LVESA and LVEDA of NF-Sham and PNOF-Sham mice did not exhibit variations after

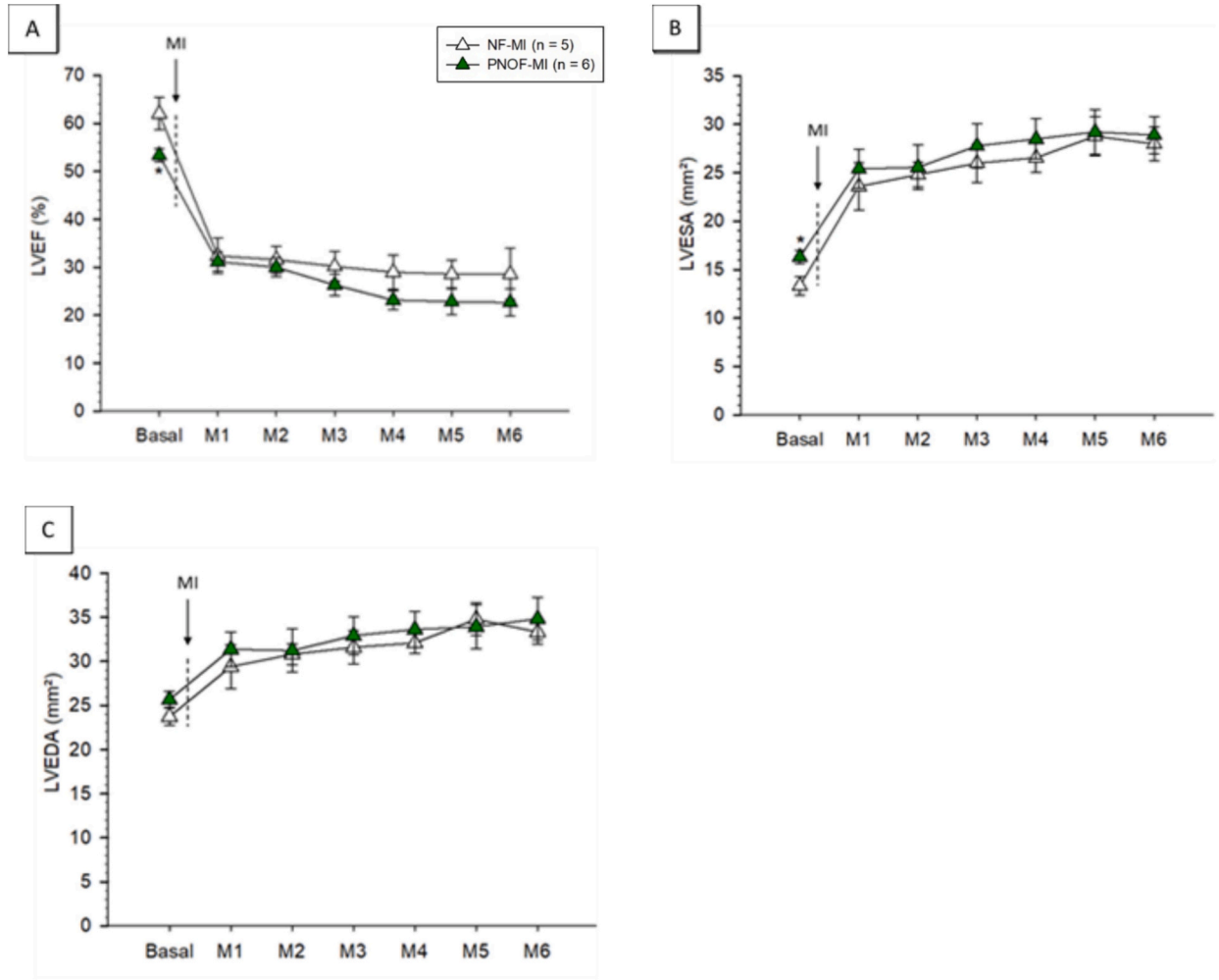

Fig. 6. (A) LVEF evolution of NF-MI and PNOF-MI mice. (B) LVESA evolution of NF-MI and PNOF-MI mice. (C) LVEDA evolution of NF-MI and PNOF-MI mice. *: significantly different from NF mice ($p < 0.05$). Two Way Repeated Measures ANOVA. LVEF, left ventricular ejection fraction; LVESA, left ventricular end-systolic area; LVEDA, left ventricular end-diastolic area.

surgery and were comparable between NF and PNOF mice (Supplementary data, Figs. S5B and C).

Basal LVEF of 4-month-old PNOF mice was significantly lower than that of NF mice (62.0 ± 3.0 % *vs* 53.3 ± 2.7 %; $p < 0.05$) (Fig. 6A). One month after MI, LVEF in NF-MI and PNOF-MI mice displayed a significant decrease compared to their basal state (32.4 ± 3.0 % and 31.7 ± 2.8 %, respectively, corresponding to a 47.7 % and 41.6 % decrease; $p < 0.05$). Subsequently, LVEF remained constituently low and stable until 6 months post-MI. No significant difference in LVEF between NF and PNOF mice were reported at any time point after surgery.

Basal LVESA of PNOF mice was significantly higher than that of NF mice (16.3 ± 2.1 mm^2 *vs* 13.3 ± 1.7 mm^2; $p < 0.05$). However, after cardiac surgery, LVESA did not differ between the two groups (Fig. 6B). Regarding LVEDA, no significant difference was observed between NF-MI and PNOF-MI mice before and after surgery (Fig. 6C).

3.5. Left ventricular systolic function

Parameters of contractile function for both NF-MI and PNOF-MI mice were monitored before and after cardiac surgery, including heart rate (HR), left ventricle end-systolic and left ventricle end-diastolic volumes (LVESV and LVEDV respectively), stroke volume (SV) and cardiac output (CO).

Systolic parameters remained unaffected by cardiac surgery in both NF-Sham and PNOF-Sham mice (Supplementary data, Table S1). Concerning left ventricular volumes, basal LVESV was increased in PNOF-MI mice compared to NF-MI mice (23.6 ± 3.0 µl *vs* 32.4 ± 2.2 µl; $p < 0.05$). After MI, both LVESV and LVEDV of NF-MI and PNOF-MI mice exhibited significant increases in comparison to their basal volumes (LVESV basal *vs* 6 months post-MI: 23.6 ± 3.0 µl *vs* 82.9 ± 9.8 µl; $p < 0.05$ in NF-MI and 32.4 ± 2.2 µl *vs* 95.5 ± 13.6 µl in PNOF-MI; $p < 0.05$. LVEDV basal *vs* 6 months post-MI: 60.9 ± 4.2 µl *vs* 115.3 ± 8.3 µl in NF-MI and 69.2 ± 3.6 µl *vs* 121.5 ± 14.1 µl in PNOF-MI; $p < 0.05$). Heart rate of PNOF-MI mice exhibited a significant increase at 2-, 3-, 5- and 6 months post-MI, whereas the HR of NF-MI mice was only significantly elevated at 1-month compared to their basal HR (Fig. 7A). Stroke volume was significantly reduced compared to the initial value in PNOF-MI mice only, persisting from 1 month up to 6 months after-MI (Fig. 7B). Cardiac output exhibited a significant decrease at 4 months and showed a trend of decrease at 6-months ($p = 0.0899$) compared to basal CO in PNOF-MI mice, whereas not such decrease was observed in NF-MI mice (Fig. 7C).

3.6. Left ventricular diastolic function

Parameters of diastolic function for NF-MI and PNOF-MI mice were measured before and after surgery, including E wave, A wave, E/A ratio and E/e′ ratio (Table 2).

Diastolic parameters were not influenced by cardiac sham surgery in both NF-Sham and PNOF-Sham mice (Supplementary data, Table S2).

E wave of NF-MI mice exhibited a significant decrease at 3-, 4-, 5- and 6-months compared to initial values, while the E wave of PNOF-MI mice was only decreased at 1-month compared to basal measurement. No significant differences were observed between the two groups, NF-MI and PNOF-MI.

A wave, E/A ratio and E/e′ ratio did not show any variation over time between NF-MI and PNOF-MI mice.

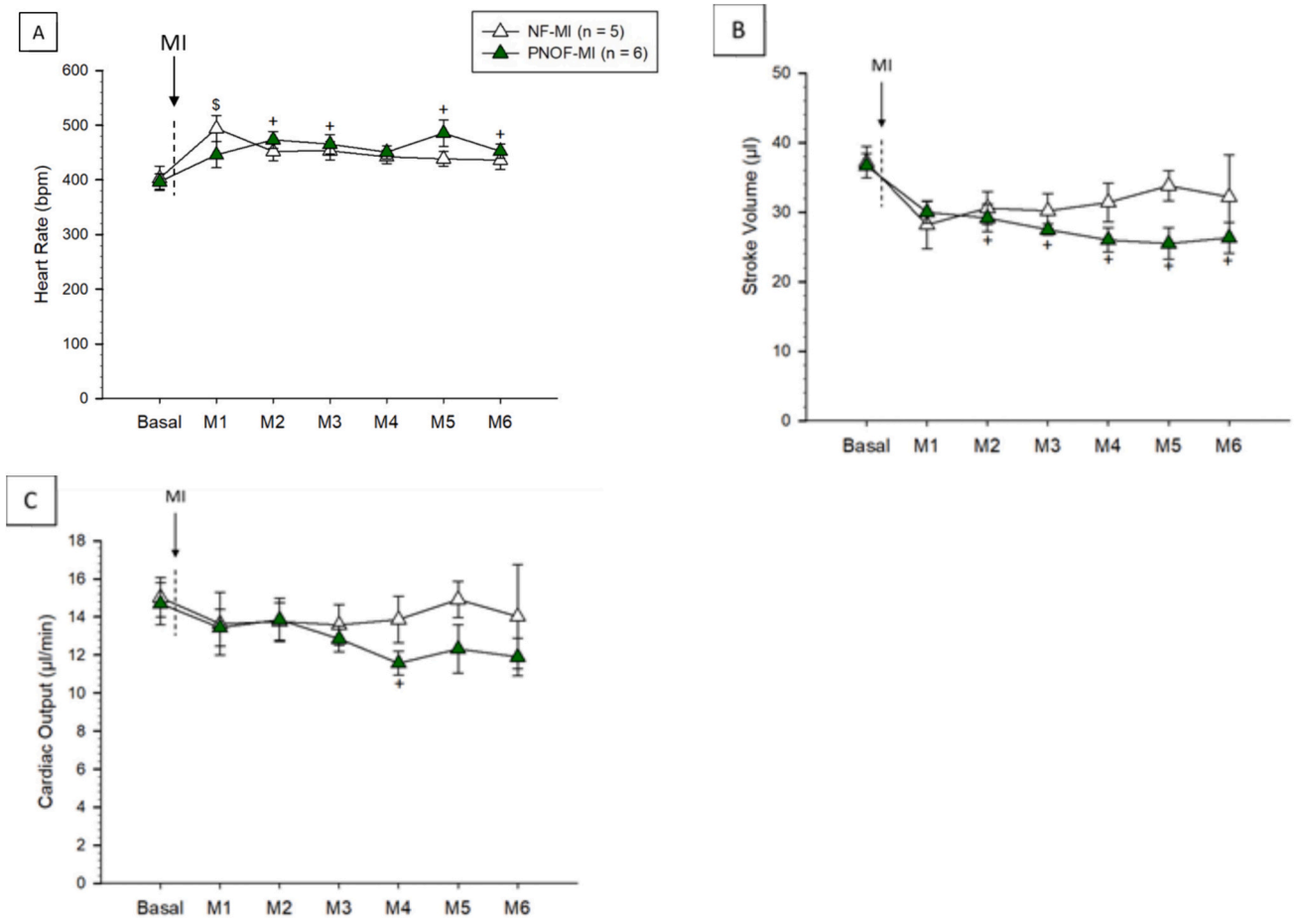

Fig. 7. (A) Heart rate evolution of NF-MI and PNOF-MI mice. (B) Stroke volume evolution of NF-MI and PNOF-MI mice. (C) Cardiac output evolution of NF-MI and PNOF-MI mice. $^{\$}$: significantly different from basal NF-MI mice ($p < 0.05$); $^{+}$: significantly different from basal PNOF-MI mice ($p < 0.05$), Two Way Repeated Measures ANOVA. HR, heart rate; SV, stroke volume; CO, cardiac output.

Table 2
Evolution of diastolic function parameters of NF-MI and PNOF-MI mice up to 6 months post-MI (n = 5 and 6 respectively).

	E wave		A wave		E/A ratio		E/e′	
	NF-MI	PNOF-MI	NF-MI	PNOF-MI	NF-MI	PNOF-MI	NF-MI	PNOF-MI
Basal	748 ± 31	734 ± 15	594 ± 46	548 ± 33	1.3 ± 0.0	1.4 ± 0.1	33.5 ± 1.0	32.9 ± 1.2
M1	688 ± 59	566 ± 27[+]	639 ± 20	507 ± 42	1.1 ± 0.1	1.1 ± 0.1	34.5 ± 8.1	45.0 ± 5.1
M2	657 ± 34	672 ± 25	630 ± 61	651 ± 46	1.1 ± 0.1	1.1 ± 0.1	43.1 ± 7.4	41.8 ± 8.0
M3	552 ± 61[$]	625 ± 52	528 ± 70	499 ± 49	1.1 ± 0.1	1.3 ± 0.2	34.8 ± 4.3	30.2 ± 3.2
M4	575 ± 40[$]	615 ± 33	552 ± 16	581 ± 38	1.1 ± 0.1	1.1 ± 0.1	37.8 ± 2.6	40.7 ± 2.2
M5	547 ± 29[$]	616 ± 10	535 ± 38	431 ± 70	1.0 ± 0.0	1.4 ± 0.2	44.3 ± 4.5	42.1 ± 7.1
M6	468 ± 82[$]	566 ± 47	509 ± 43	600 ± 20	1.0 ± 0.1	1.0 ± 0.1	36.8 ± 4.4	37.8 ± 6.0

Results are expressed as mean ± SEM.
[$] Significantly different from basal NF-MI mice ($p < 0.05$).
[+] Significantly different from basal PNOF-MI mice ($p < 0.05$), Two Way Repeated Measures ANOVA.

3.7. Organ mass and interstitial fibrosis

The evaluation of plasma cardiac troponin I (cTnI) revealed an elevation in cTnI levels in MI-operated mice compared to sham-operated mice from both groups, 24 h after surgery (Supplementary data, Fig. S6A). Plasma cTnI level was significantly increased in PNOF-Sham mice compared to NF-Sham mice, but it was not significantly different between NF-MI mice and PNOF-MI mice.

Myocardial infarction induced an increase in cardiac mass, as evidenced by the elevation of left ventricle mass-to-tibia length ratio in MI-

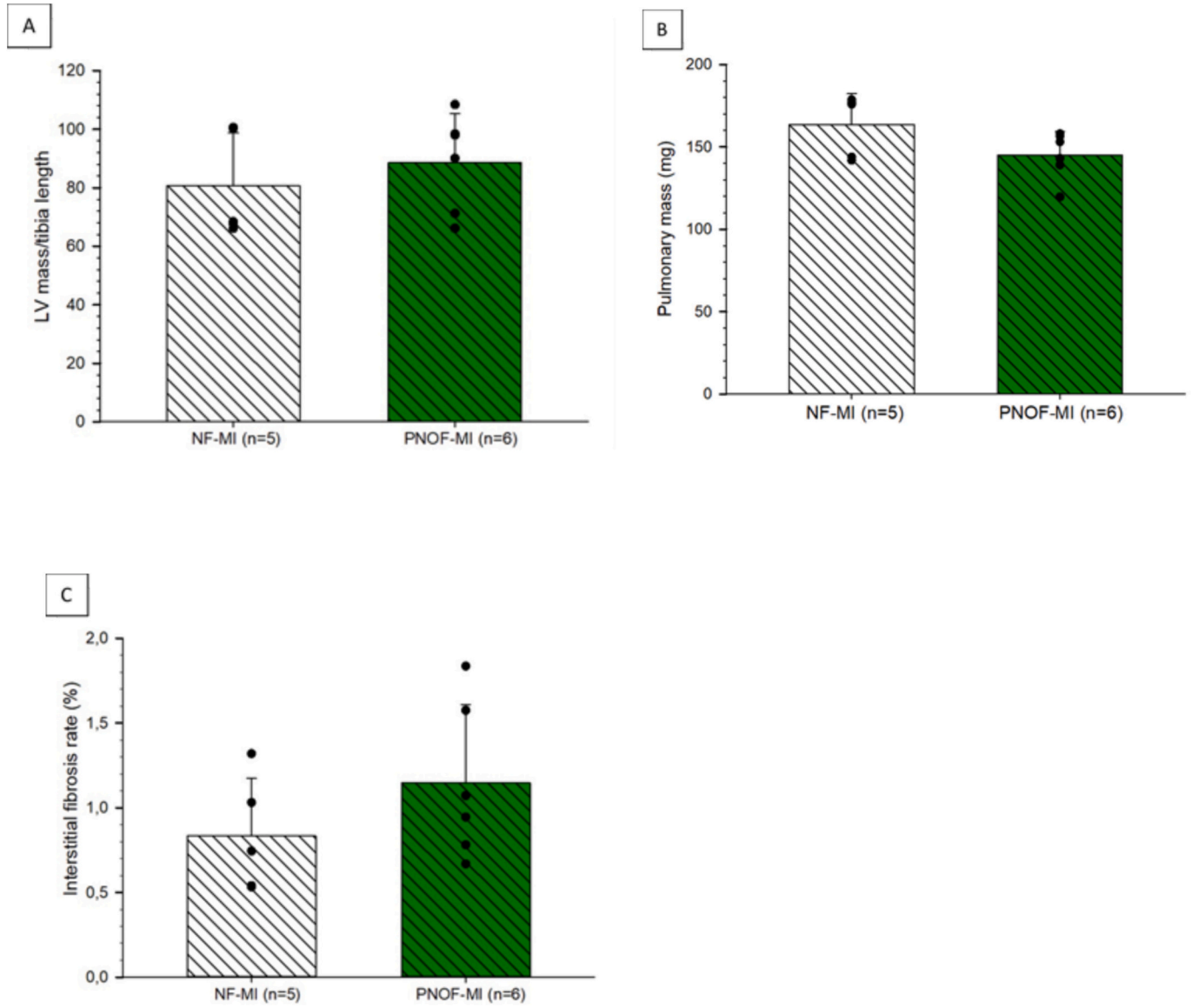

Fig. 8. (A) Cardiac mass represented as the left ventricular-to-tibia length ratio of NF-MI and PNOF-MI at 6-months post-MI. (B) Lung mass of NF-MI and PNOF-MI at 6 months post-MI. (C) Cardiac interstitial fibrosis rate in the remote zone of NF-MI and PNOF-MI 6 months post-MI. LV mass, left ventricular mass.

operated mice compared to sham-operated mice (Supplementary data, Fig. S6B). However, there was no significant difference in lung mass between MI-operated and sham-operated mice (Supplementary data, Fig. S6C).

After 6 months, cardiac mass in NF-MI and PNOF-MI did not show a significant difference (Fig. 8A). In addition, cardiomyocyte cross sectional area was measured in the remote zone by WGA histological staining but it did not reveal any difference between the two groups (data not shown). Similarly, lung mass was measured and was not found to be different between the two groups (Fig. 8B).

Histological analysis was conducted to evaluate the presence of interstitial fibrosis in the remote zone of hearts at 6 months post-MI. Sirius red staining did not reveal any significant difference in cardiac collagen deposition between NF-MI and PNOF-MI group (Fig. 8C).

3.8. Cardiac gene expression

The cardiac expression of genes associated with heart failure, namely β-MHC, ANF and BNP, cTnT and collagen 1α1 and 1α2, was assessed 2- and 6-months post-MI in the RZ and IZ of both NF and PNOF mice. Two months after surgery, there were no changes in natriuretic peptides and β-MHC gene expression in the RZ of NF-MI and PNOF-MI mice compared to NF-Sham mice. However, their expressions were all increased in the IZ (Supplementary data, Fig. S7A). The cardiac expression of collagen 1α1 and 1α2 was only significantly increased in the RZ of PNOF-MI mice, but it was elevated in both NF-MI and PNOF-MI mice compared to sham-operated mice in the IZ (Supplementary data, Fig. S7B). Regarding the expression of cardiac troponin T, it did not differ in all groups regardless of the cardiac zones (Supplementary data, Fig. S7C). Regarding the comparison between NF-MI and PNOF-MI mice at 6 months post-MI, there were no differences in the expression of β-MHC, ANF and BNP (Fig. 9A) as well as collagen 1α1 and 1α2 (Fig. 9B), both in the RZ and the IZ. There was no significant difference in cardiac troponin T expression in the IZ; however, PNOF-MI mice demonstrated a trend of cTnt expression decrease in the RZ compared to NF-MI mice ($p = 0.0706$) (Fig. 9C).

4. Discussion

To the best of our knowledge, this study was the first to assess how a permanent MI, leading to chronic heart failure, may distinctly impact the hearts of mice showing overweight and cardiac dysfunction that were “programmed” through postnatal overfeeding, in comparison to their control littermates.

Few preclinical experimental models offer the possibility to comprehensively explore the multifaceted aspects of CV risk factors encountered in clinical settings. Patients developing post-MI heart failure often have a history of CV diseases, are frequently overweight or obese, hypertensive, exhibit dyslipidaemia, T2 diabetes and are in their middle age [30]. Indeed, adult mice submitted to a short-term period of overfeeding after birth display long-lasting features of metabolic syndrome, with increased risk of cardiac alteration and heightened sensitivity to myocardial infarction [13]. Our experimental model significantly differs from classical models of diabetic/obese mice induced by genetic mutations (ob/ob or db/db mouse) or high fat/high sucrose diets, which do not capture the multidimensional aspects of metabolic syndrome in humans. From the young-adult (4 months) to old ages (12 months), PNOF mice exhibit overweight with increased

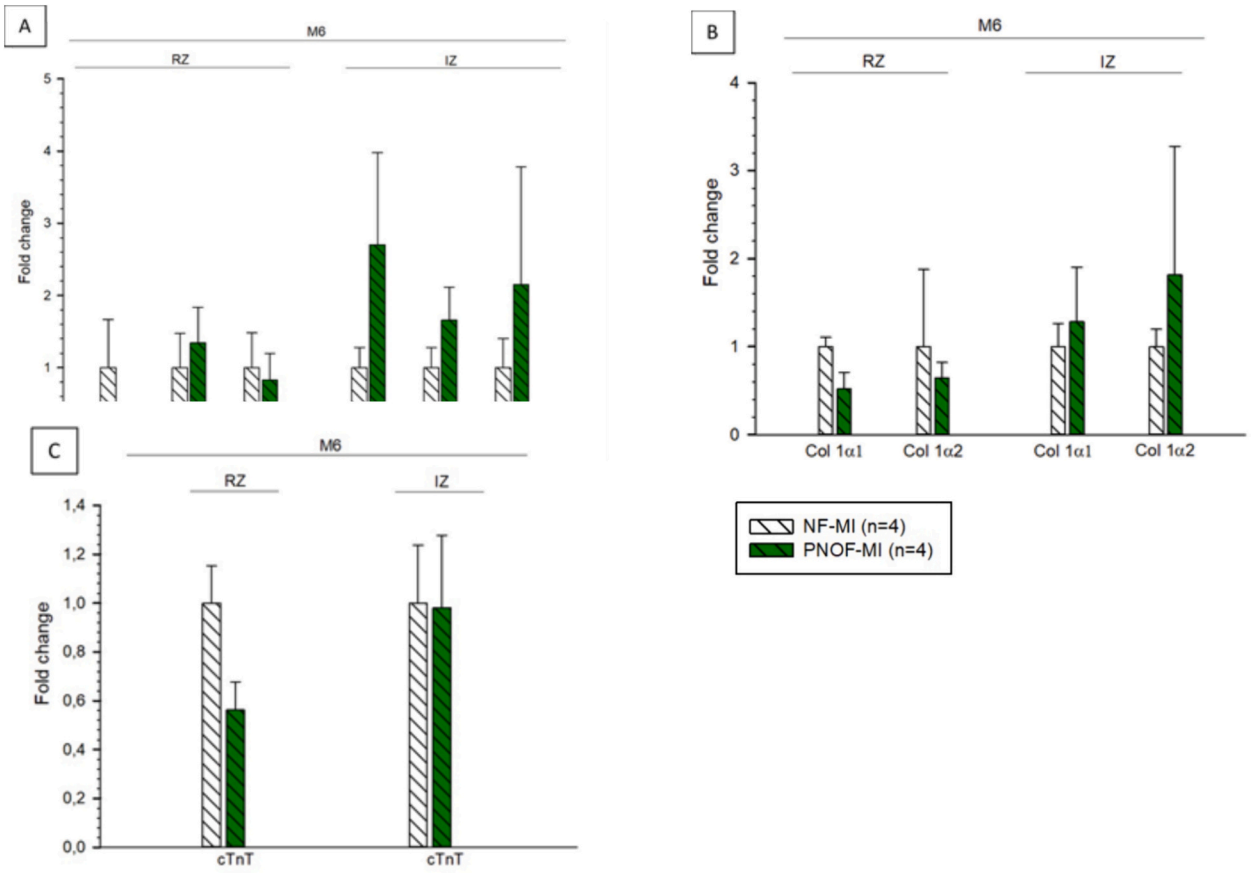

Fig. 9. Cardiac mRNA expression of NF-MI and PNOF-MI mice at 6-months post-MI, in the remote and infarcted zones (A) β-MHC, ANF and BNP (B) Collagen 1α1 and 1α2 (C) Cardiac troponin T. Results are expressed as fold change (2-ΔΔCT) over the levels of NF-MI. ANF, atrial natriuretic factor; BNP, brain natriuretic peptide; β-MHC, β-Myosin Heavy Chain; Col1α1, collagen 1α1; Col1α2, collagen 1α2; cTnT, cardiac troponin T; RZ, remote zone; IZ, infarcted zone.

adiposity, glucose intolerance/insulin resistance, moderately reduced left ventricular contractility, and increased infarct size after experimental myocardial ischemia-reperfusion injury [15,31]. In the present study, we utilized 4-month-old mature mice and, prior to cardiac surgery, PNOF mice displayed an 8 % to 15 % increase in body weight. This moderate overweight is consistent with previous studies from our group and others, with some variations that may be attributed to the number of pups per mother or different strains [9,15,27,32]. The body overweight of PNOF mice remained unchanged after MI-surgery, except transiently, which could be influenced by the small group sizes. Moreover, in a separate group of animals, we also evidenced that 4-month-old PNOF mice showing a similar increase in body weight displayed an alteration of glucose tolerance. This impairment was recently described in a study from our laboratory in PNOF mice aged 4, 6, and 12 months, along with altered insulin tolerance [33].

Myocardial infarction resulted in a significant decrease of LVEF in both NF-MI and PNOF-MI, observed as early as 7 days post-MI, indicating a rapid and substantial deterioration of the systolic function. Surprisingly, postnatal overnutrition did not exacerbate the decline in LVEF. Previous studies from our team revealed that hearts from PNOF mice or rats showed increased susceptibility to ischemia-reperfusion injury, as demonstrated by impaired myocardial contractility after 30 min of ischemia [8,9,34], coupled with increased infarct size [10,15,27] and associated with a reduced expression of cardioprotective pathways PI3K/Akt and STAT3 [33]. Based on these results, we expected to observe a more pronounced reduction in LVEF in PNOF mice following MI. In addition, other parameters such as LV volumes and areas were affected by MI, inducing an increase in LVESA and LVEDA. These changes are characteristic of contractile dysfunction associated with ventricular dilation, key components of cardiac remodelling reported in other studies evaluating cardiac function post-MI [35–38]. Interestingly, a significant increase in basal LVESA and consequently basal LVESV was noted in PNOF mice compared to the NF control group. However, similar to LVEF this difference was not sustained after surgery.

Nevertheless, while ejection fraction is among one of the most commonly used parameters for assessing cardiac contractile function, other parameters related to cardiac contraction displayed significant changes. First, we observed a significant decrease in stroke volume (SV) associated with a significant heart rate (HR) increase in PNOF-MI mice, compared to their initial values. Although cardiac output (CO) was initially maintained the first 3 months, it was significantly decreased at some points. Stroke volume is determined by contractility, preload and afterload, factors that are partially affected by peripheral vascular tone, blood volume, wall stress or neurohormonal factors. During cardiac remodelling, ventricular dilation, hypertrophy, and neurohormonal systems activation such as the renin-angiotensin-aldosterone (RAA) or sympathetic nervous (SN) systems contribute to maintaining stroke volume and cardiac output by increasing preload. Vasoconstriction through RAA and SN systems also helps maintaining an adequate organ perfusion [39]. However, prolonged stimulation of these neurohormonal systems over time can lead to sustained vasoconstriction and increase in afterload, contributing to the progression the of heart failure [40]. Moreover, previous observations have indicated increased blood pressure and altered vascular reactivity in PNOF animals [14,15,41,42], potentially explaining why PNOF mice failed to sustain a stable CO. Additionally, previous reports have highlighted renal dysfunction in PNOF animals [43,44], along with altered contractile response to angiotensin II and changes in gene expression of components of the RAAS in both the kidney [45] and the heart [34].

Interestingly, 6-months after MI, the expression of cardiac troponin T showed a trend of decreased expression in the RZ of PNOF-MI mice compared to NF-MI mice. This reduction may indicate underlying cardiac cell death in the hearts of PNOF-MI mice, potentially contributing to a decreased myocardial contractility. Previous studies have demonstrated that PNOF rat hearts exhibit reduced contractility *ex vivo* with an increased expression of the apoptotic marker caspase 8 [34]. Therefore, an elevated rate of cardiomyocyte death within the hearts of PNOF mice could play a role in reducing SV through reduced cardiac contractility.

As observed in previous studies [36,38,46], the cardiac expressions of ANF and BNP genes were increased in the IZ of both NF-MI and PNOF-MI mice as compared to sham mice, 2 months after surgery. During the progression of heart failure, natriuretic peptides such as ANF and BNP are expressed and exert vasodilatory, diuretic and natriuretic actions. Along with β-MHC, they are predominantly expressed during the foetal period but a phenomenon of "foetal gene reprogramming" is observed in heart failure. As for adverse cardiac remodelling, this process is considered detrimental for the heart [47,48]; however, our study did not reveal any differences in cardiac mRNA expression of ANF, BNP and β-MHC between NF-MI and PNOF-MI mice did at 2 and 6 months in the two zones.

Cardiac hypertrophy is an essential compensatory mechanism for maintaining cardiac function after myocardial infarction. However, excessive hypertrophy also contributes to adverse remodelling and deterioration of cardiac function [49]. In our study, the LV mass-to-tibia length ratio from PNOF-MI and NF-MI mice was increased compared to their respective sham groups at 2 months, demonstrating the heart's adaptation to myocardial infarction. However, it was not different between the two MI groups at 2 and 6 months, similarly to the hypertrophic marker β-MHC, and to cardiomyocyte cross-sectional area. Staining for interstitial fibrosis and collagen mRNA expression in both the remote and infarcted zones were also comparable in NF-MI and PNOF-MI mice. Despite previous studies reporting higher cardiac hypertrophy and fibrosis in hearts of PNOF mice and rats [9,14–16,50,51], none of them were conducted in a context of post-MI cardiac remodelling where the structure of the heart is known to be completely rearranged [52].

Finally, impaired glucose tolerance in PNOF mice further highlighted the impact of postnatal overfeeding on glucose metabolism. During cardiac remodelling and heart failure development, glucose handling is known to undergo significant changes such as an increase in glucose uptake and glycolysis [53,54]. Therefore, metabolic disturbances in the hearts of PNOF mice cannot be excluded.

While these results are promising, they still present some limitations. First, additional data would be helpful to explain the underlying mechanisms behind these observations. Furthermore, given the significant sex disparities observed in both experimental studies and clinical settings, a similar study should be conducted on NF and PNOF female mice. [55,56]. Our laboratory demonstrated that PNOF female mice also have increased cardiac sensitivity to ischemia-reperfusion injury as well as metabolic alterations (unpublished data).

In conclusion, this study provides the first evidence of increased cardiac sensitivity to adverse cardiac remodelling following myocardial infarction in postnatally overfed mice. While NF-MI mice maintained a compensated heart failure state after MI, PNOF-MI mice exhibited a worsening of their cardiac function, initially marked by a decrease in SV followed by a decline in CO starting at 4-months post-MI. Although other mechanisms may be involved and require further investigation, this greater cardiac sensitivity could be partially attributed to increased myocardial cell death, resulting in reduced cardiac contractility, an early sign of heart failure decompensation. It is therefore essential to adjust litter size in rodent's groups in experimental studies aiming at evaluating cardiovascular pathological conditions [57].

Funding

This work was supported by the Association de Cardiologie de Bourgogne, and by grants from the Regional Council of Bourgogne-Franche-Comté, the French Ministry of Research and Education, the University of Burgundy, the Fédération Française de Cardiologie and the Fondation de France. This work was supported by the "Délégation Régionale Academique à la Recherche et à l'innovation" (DRADI) through the CPER IDATHERAP project (n° BFCO-SR-P541).

CRediT authorship contribution statement

Marie Josse: Writing – original draft, Methodology, Investigation, Formal analysis, Data curation. **Eve Rigal:** Validation, Methodology, Investigation. **Nathalie Rosenblatt-Velin:** Writing – review & editing, Supervision. **Bertrand Collin:** Resources. **Geoffrey Dogon:** Investigation. **Luc Rochette:** Validation. **Marianne Zeller:** Writing – review & editing. **Catherine Vergely:** Writing – review & editing, Supervision, Project administration, Funding acquisition, Data curation, Conceptualization.

Declaration of competing interest

The authors declare no conflict of interests.

Data availability

Data will be made available on request.

Acknowledgments

The authors gratefully thank Ivan Porcherot and Sandy Guner for technical assistance, and Marie Thauvin for her involvement in histological experiments. The authors also gratefully thank Gilles Renault and his team for the lend of a 30 MHz transducer.

Appendix A. Supplementary data

Supplementary data to this article can be found online at https://doi.org/10.1016/j.bbadis.2024.167516.

References

[1] K.M. Godfrey, R.M. Reynolds, S.L. Prescott, M. Nyirenda, V.W. Jaddoe, J. G. Eriksson, B.F. Broekman, Influence of maternal obesity on the long-term health of offspring, Lancet Diabetes Endocrinol. 5 (2017) 53–64.
[2] J. Yan, L. Liu, Y. Zhu, G. Huang, P.P. Wang, The association between breastfeeding and childhood obesity: a meta-analysis, BMC Public Health 14 (2014) 1267.
[3] D. Gniuli, A. Calcagno, M.E. Caristo, A. Mancuso, V. Macchi, G. Mingrone, R. Vettor, Effects of high-fat diet exposure during fetal life on type 2 diabetes development in the progeny, J. Lipid Res. 49 (2008) 1936–1945.
[4] S.E. King, M.K. Skinner, Epigenetic transgenerational inheritance of obesity susceptibility, Trends Endocrinol. Metab. 31 (2020) 478–494.
[5] P.D. Gluckman, M.A. Hanson, T. Buklijas, A conceptual framework for the developmental origins of health and disease, J. Dev. Orig. Health Dis. 1 (2010) 6–18.
[6] Y. Arima, H. Fukuoka, Developmental origins of health and disease theory in cardiology, J. Cardiol. 76 (2020) 14–17.
[7] A. Habbout, N. Li, L. Rochette, C. Vergely, Postnatal overfeeding in rodents by litter size reduction induces major short- and long-term pathophysiological consequences, J. Nutr. 143 (2013) 553–562.
[8] A. Habbout, S. Delemasure, F. Goirand, J.C. Guilland, F. Chabod, M. Sediki, L. Rochette, C. Vergely, Postnatal overfeeding in rats leads to moderate overweight and to cardiometabolic and oxidative alterations in adulthood, Biochimie 94 (2012) 117–124.
[9] A.K. Vieira, V.M. Soares, A.F. Bernardo, F.A. Neves, A.B. Mattos, R.M. Guedes, E. Cortez, D.C. Andrade, G. Lacerda-Miranda, E.P. Garcia-Souza, A.S. Moura, Overnourishment during lactation induces metabolic and haemodynamic heart impairment during adulthood, Nutr. Metab. Cardiovasc. Dis. 25 (2015) 1062–1069.
[10] C. de Moura Freitas, L. Nascimento, G.R.F. Braz, S.C. Andrade-Silva, N.C. Lima-Junior, T. de Araujo Silva, M.P. Fernandes, D.J.S. Ferreira, C.J. Lagranha, Mitochondrial impairment following neonatal overfeeding: a comparison between normal and ischemic-reperfused hearts, J. Cell. Biochem. 120 (2019) 7341–7352.
[11] G. Sanchez-Garcia, L. Del Bosque-Plata, E. Hong, Postnatal overnutrition affects metabolic and vascular function reflected by physiological and histological changes in the aorta of adult Wistar rats, Clin. Exp. Hypertens. 40 (2018) 452–460.
[12] D. Gonzalez-Hedstrom, L. Guerra-Menendez, A. Tejera-Munoz, S. Amor, M. de la Fuente-Fernandez, B. Martin-Carro, R. Arriazu, A.L.L. Garcia-Villalon, M. Granado, Overfeeding during lactation in rats is associated with cardiovascular insulin resistance in the short-term, Nutrients 12 (2020).
[13] M. Josse, E. Rigal, N. Rosenblatt-Velin, L. Rochette, M. Zeller, C. Guenancia, C. Vergely, Programming of cardiovascular dysfunction by postnatal overfeeding in rodents, Int. J. Mol. Sci. 21 (2020).
[14] M.D.F. Junior, K.V.N. Cavalcante, L.A. Ferreira, P.R. Lopes, C.N.R. Pontes, A.S. M. Bessa, A.R. Neves, F.A. Francisco, G.R. Pedrino, C.H. Xavier, P.C.F. Mathias, C. H. Castro, R.M. Gomes, Postnatal early overfeeding induces cardiovascular dysfunction by oxidative stress in adult male Wistar rats, Life Sci. 226 (2019) 173–184.
[15] A. Habbout, C. Guenancia, J. Lorin, E. Rigal, C. Fassot, L. Rochette, C. Vergely, Postnatal overfeeding causes early shifts in gene expression in the heart and long-term alterations in cardiometabolic and oxidative parameters, PLoS One 8 (2013) e56981.
[16] G.A. de Araujo, R.D.S. Farias, S.S. Pedro, N.N. Rocha, F.C.F. Brito, C.B. V. Scaramello, Overweight during lactation and its implications for biometric, nutritional and cardiovascular parameters of young and adult male and female rats, J. Nutr. Sci. 9 (2020) e27.
[17] I. Csige, D. Ujvarosy, Z. Szabo, I. Lorincz, G. Paragh, M. Harangi, S. Somodi, The impact of obesity on the cardiovascular system, J. Diabetes Res. 2018 (2018) 3407306.
[18] S. Mottillo, K.B. Filion, J. Genest, L. Joseph, L. Pilote, P. Poirier, S. Rinfret, E. L. Schiffrin, M.J. Eisenberg, The metabolic syndrome and cardiovascular risk a systematic review and meta-analysis, J. Am. Coll. Cardiol. 56 (2010) 1113–1132.
[19] S.D. Prabhu, N.G. Frangogiannis, The biological basis for cardiac repair after myocardial infarction: from inflammation to fibrosis, Circ. Res. 119 (2016) 91–112.
[20] J.B. Oliveira, A. Soares, A.C. Sposito, Inflammatory response during myocardial infarction, Adv. Clin. Chem. 84 (2018) 39–79.
[21] J.J. Gajarsa, R.A. Kloner, Left ventricular remodeling in the post-infarction heart: a review of cellular, molecular mechanisms, and therapeutic modalities, Heart Fail. Rev. 16 (2011) 13–21.
[22] H. Venugopal, A. Hanna, C. Humeres, N.G. Frangogiannis, Properties and functions of fibroblasts and myofibroblasts in myocardial infarction, Cells 11 (2022).
[23] A. Galli, F. Lombardi, Postinfarct left ventricular remodelling: a prevailing cause of heart failure, Cardiol. Res. Pract. 2016 (2016) 2579832.
[24] N.S. Dhalla, S. Rangi, A.P. Babick, S. Zieroth, V. Elimban, Cardiac remodeling and subcellular defects in heart failure due to myocardial infarction and aging, Heart Fail. Rev. 17 (2012) 671–681.
[25] D. Snipelisky, S.P. Chaudhry, G.C. Stewart, The many faces of heart failure, Card. Electrophysiol. Clin. 11 (2019) 11–20.
[26] C. Guenancia, O. Hachet, M. Aboutabl, N. Li, E. Rigal, Y. Cottin, L. Rochette, C. Vergely, Overweight in mice, induced by perinatal programming, exacerbates doxorubicin and trastuzumab cardiotoxicity, Cancer Chemother. Pharmacol. 77 (2016) 777–785.
[27] N. Li, C. Guenancia, E. Rigal, O. Hachet, P. Chollet, L. Desmoulins, C. Leloup, L. Rochette, C. Vergely, Short-term moderate diet restriction in adulthood can reverse oxidative, cardiovascular and metabolic alterations induced by postnatal overfeeding in mice, Sci. Rep. 6 (2016) 30817.
[28] M.M. Dann, S.Q. Clark, N.A. Trzaskalski, C.C. Earl, L.E. Schepers, S.M. Pulente, E. N. Lennord, K. Annamalai, J.M. Gruber, A.D. Cox, I. Lorenzen-Schmidt, R. Seymour, K.H. Kim, C.J. Goergen, E.E. Mulvihill, Quantification of murine myocardial infarct size using 2-D and 4-D high-frequency ultrasound, Am. J. Physiol. Heart Circ. Physiol. 322 (2022) H359–H372.
[29] A.C. Bon-Mathier, T. Deglise, S. Rignault-Clerc, C. Bielmann, L. Mazzolai, N. Rosenblatt-Velin, Brain natriuretic peptide protects cardiomyocytes from apoptosis and stimulates their cell cycle re-entry in mouse infarcted hearts, Cells 12 (2022).
[30] J.D. Tune, A.G. Goodwill, D.J. Sassoon, K.J. Mather, Cardiovascular consequences of metabolic syndrome, Transl. Res. 183 (2017) 57–70.
[31] L.L. Souza, E.G. Moura, P.C. Lisboa, Litter size reduction as a model of overfeeding during lactation and its consequences for the development of metabolic diseases in the offspring, Nutrients 14 (2022).
[32] G. Collden, E. Caron, S.G. Bouret, Neonatal leptin antagonism improves metabolic programming of postnatally overnourished mice, Int. J. Obes. 46 (2022) 1138–1144.
[33] E. Rigal, M. Josse, C. Greco, N. Rosenblatt, L. Rochette, C. Guenancia, C. Vergely, Short-term postnatal overfeeding induces long-lasting cardiometabolic syndrome in mature and old mice associated with increased sensitivity to myocardial infarction, Mol. Nutr. Food Res. 68 (2024) e2400136.
[34] M. Granado, N. Fernandez, L. Monge, G. Carreno-Tarragona, J.C. Figueras, S. Amor, A.L. Garcia-Villalon, Long-term effects of early overnutrition in the heart of male adult rats: role of the renin-angiotensin system, PLoS One 8 (2014) e65172.
[35] S. Kanno, D.L. Lerner, R.B. Schuessler, T. Betsuyaku, K.A. Yamada, J.E. Saffitz, A. Kovacs, Echocardiographic evaluation of ventricular remodeling in a mouse model of myocardial infarction, J. Am. Soc. Echocardiogr. 15 (2002) 601–609.
[36] H. Bayat, J.S. Swaney, A.N. Ander, N. Dalton, B.P. Kennedy, H.K. Hammond, D. M. Roth, Progressive heart failure after myocardial infarction in mice, Basic Res. Cardiol. 97 (2002) 206–213.
[37] C. Benavides-Vallve, D. Corbacho, O. Iglesias-Garcia, B. Pelacho, E. Albiasu, S. Castano, A. Munoz-Barrutia, F. Prosper, C. Ortiz-de-Solorzano, New strategies for echocardiographic evaluation of left ventricular function in a mouse model of long-term myocardial infarction, PLoS One 7 (2012) e41691.
[38] F. Sam, D.B. Sawyer, D.L. Chang, F.R. Eberli, S. Ngoy, M. Jain, J. Amin, C. S. Apstein, W.S. Colucci, Progressive left ventricular remodeling and apoptosis late after myocardial infarction in mouse heart, Am. J. Physiol. Heart Circ. Physiol. 279 (2000) H422–H428.
[39] E. Tanai, S. Frantz, Pathophysiology of heart failure, comprehensive, Physiology 6 (2015) 187–214.
[40] J. Hartupee, D.L. Mann, Neurohormonal activation in heart failure with reduced ejection fraction, Nat. Rev. Cardiol. 14 (2017) 30–38.
[41] V. Achard, C. Sanchez, V. Tassistro, M. Verdier, M.C. Alessi, M. Grino, Immediate postnatal overfeeding in rats programs aortic wall structure alterations and

metalloproteinases dysregulation in adulthood, Am. J. Hypertens. 29 (2016) 719–726.
[42] C. Juvet, B. Siddeek, C. Yzydorczyk, C. Vergely, K. Nardou, J.B. Armengaud, M. Benahmed, U. Simeoni, F. Cachat, H. Chehade, Renal programming by transient postnatal overfeeding: the role of senescence pathways, Front. Physiol. 11 (2020) 511.
[43] H.E. Yim, K.S. Ha, I.S. Bae, K.H. Yoo, Y.S. Hong, J.W. Lee, Overweight, hypertension and renal dysfunction in adulthood of neonatally overfed rats, J. Nutr. Biochem. 24 (2013) 1324–1333.
[44] F. Boubred, L. Daniel, C. Buffat, J.M. Feuerstein, M. Tsimaratos, C. Oliver, F. Dignat-George, M. Lelievre-Pegorier, U. Simeoni, Early postnatal overfeeding induces early chronic renal dysfunction in adult male rats, Am. J. Physiol. Ren. Physiol. 297 (2009) F943–F951.
[45] M. Granado, S. Amor, N. Fernandez, G. Carreno-Tarragona, M.C. Iglesias-Cruz, B. Martin-Carro, L. Monge, A.L. Garcia-Villalon, Effects of early overnutrition on the renal response to Ang II and expression of RAAS components in rat renal tissue, Nutr. Metab. Cardiovasc. Dis. 27 (2017) 930–937.
[46] K. Fujisue, K. Sugamura, H. Kurokawa, J. Matsubara, M. Ishii, Y. Izumiya, K. Kaikita, S. Sugiyama, Colchicine improves survival, left ventricular remodeling, and chronic cardiac function after acute myocardial infarction, Circ. J. 81 (2017) 1174–1182.
[47] H. Taegtmeyer, S. Sen, D. Vela, Return to the fetal gene program: a suggested metabolic link to gene expression in the heart, Ann. N. Y. Acad. Sci. 1188 (2010) 191–198.
[48] A. van der Pol, M.F. Hoes, R.A. de Boer, P. van der Meer, Cardiac foetal reprogramming: a tool to exploit novel treatment targets for the failing heart, J. Intern. Med. 288 (2020) 491–506.
[49] S.A. Leanca, D. Crisu, A.O. Petris, I. Afrasanie, A. Genes, A.D. Costache, D. N. Tesloianu, I.I. Costache, Left ventricular remodeling after myocardial infarction: from physiopathology to treatment, Life (Basel) 12 (2022).
[50] L. Chavaglia Cavalet, L.C. Dos Santos Ribeiro, G.B. Rosa, K.K. Sousa, A.B.S. de Melo, D.B.T. Campos, L.A. Ferreira, N.O. Amaral, Y.T.V. Calisto, A.G. de Castro, C. H. de Castro, G.R. Pedrino, R.M. Gomes, Long-term effects of early overfeeding and food restriction during puberty on cardiac remodeling in adult rats, J. Dev. Orig. Health Dis. 11 (2020) 492–498.
[51] A.F. Bernardo, E. Cortez, F.A. Neves, A.K. Vieira, M. Soares Vde, A.C. Rodrigues-Cunha, D.C. Andrade, A.A. Thole, D. Gabriel-Costa, P.C. Brum, A.S. Moura, E. P. Garcia-Souza, Overnutrition during lactation leads to impairment in insulin signaling, up-regulation of GLUT1 and increased mitochondrial carbohydrate oxidation in heart of weaned mice, J. Nutr. Biochem. 29 (2016) 124–132.
[52] Q.Q. Wu, Y. Xiao, Y. Yuan, Z.G. Ma, H.H. Liao, C. Liu, J.X. Zhu, Z. Yang, W. Deng, Q.Z. Tang, Mechanisms contributing to cardiac remodelling, Clin. Sci. (Lond.) 131 (2017) 2319–2345.
[53] G.D. Lopaschuk, Q.G. Karwi, R. Tian, A.R. Wende, E.D. Abel, Cardiac energy metabolism in heart failure, Circ. Res. 128 (2021) 1487–1513.
[54] A.A. Gibb, B.G. Hill, Metabolic coordination of physiological and pathological cardiac remodeling, Circ. Res. 123 (2018) 107–128.
[55] M.K. Mahowald, K. Esmail, F.M. Ezzeddine, C. Choi, H. Mieszczanska, G. Velarde, Sex disparities in cardiovascular disease, Methodist Debakey Cardiovasc. J. 20 (2024) 107–119.
[56] S. Mahmoodzadeh, D. Fliegner, E. Dworatzek, Sex differences in animal models for cardiovascular diseases and the role of estrogen, Handb. Exp. Pharmacol. (2012) 23–48.
[57] M. Parra-Vargas, S.G. Bouret, J.C. Bruning, E.G. de Moura, T. Garland Jr., P. C. Lisboa, S.E. Ozanne, M.E. Patti, A. Plagemann, J.R. Speakman, M. Tena-Sempere, C. Vergely, L.M. Zeltser, J.C. Jimenez-Chillaron, The long-lasting shadow of litter size in rodents: litter size is an underreported variable that strongly determines adult physiology, Mol. Metab. 71 (2023) 101707.